

Synthesis and characterization of HAp/MgPO₄ Nanocomposites from Green Mussel Shell as potential adsorbent

*Aura Gitta Zhafirah*¹, *Dika Putra Wijaya*¹, *Elsa Putri Rahmawati*¹, *Marshya Qurrotul Aini Wibowo*¹, *Nilna Inayatan Nafiah*¹, *Putri Azzahra*¹, *Etika Sholichatus Zahroh*¹, *Yoshie Stephanie*¹, and *Danar Danar*^{1,1}

¹Universitas Negeri Malang, Chemistry Department, 65145, Malang, Indonesia

Abstract. This study aimed to synthesis and characterization material HAp/MgPO₄ as an adsorbent for wastewater analysis using the precipitation method on green mussel shell waste (biogenic Ca source) and characterized by XRD, FTIR, SEM-EDX, UV-Vis and AAS. Calcination at 800-1000 °C yielded a pure HAp phase (COD 9011091) with increasing crystallinity at higher temperature (95.86 %). FTIR confirmed HAp characteristic bands (PO₄³⁻, OH⁻) and some carbonate inclusion, indicating successful HAp formation. SEM-EDX revealed porous aggregates (4-100 nm) with a dominant Ca, P, Mg, O composition. XRF of raw shells showed Ca 96.3 %, rising to 98.6 % CaO after calcination. AAS measurements of filtrate showed Ca²⁺ release of 56.7, 154.1, and 50.1 ppm for samples calcined at 800, 900, and 1000 °C (highest at 900 °C). The results of UV-Vis measurements showed that the absorbance (A) and concentration (ppm) values changed with increasing temperature. At 800°C, the highest absorbance value was 1.28 with a concentration of 0.332 ppm, while at 900°C the absorbance value decreased to 1.11 with a concentration of 0.287 ppm. At 1000 °C, the absorbance value increased slightly to 1.12 with a concentration of 0.290 ppm. These structural features suggest effective adsorption of Fe²⁺/Ni²⁺. Green mussel-derived HAp/MgPO₄ thus offers an eco-friendly, high-purity adsorbent.

Keywords: Green mussel shell, HAp/MgPO₄, precipitation method, variation calcination temperature, and potential adsorbent.

1 Introduction

Heavy metals are among the chemicals that are frequently discovered in industrial wastewaters. They are often created by industrial processes, such as mining, electrical industries such as paint, papermaking, tanning, metal smelting, textiles & dyes, insecticides,

¹ Corresponding author: danar.fmipa@um.ac.id

and fertilizers [1]. An important cause of environmental concern is the enrichment of these heavy metals and dyes through careless discharges that go over allowable limits, which poses a severe risk to human health and the environment [2], [3]. Adsorption is one of the techniques that have been documented for the treatment of effluents including heavy metals [4], [5]. Industrial progress in a country can be a benchmark for its economic progress [6]. However, environmental pollution caused by industry is also unavoidable, one of which is heavy metal contamination [7]. This problem often plays a dominant role in the emergence of environmental pollution caused by heavy metals. Heavy metals in normal amounts or thresholds that do not exceed the provisions set by the local government play a role in regulating heavy metal contamination. However, if these levels exceed the threshold set by the government, heavy metals become environmental pollutants that are toxic to the body and the environment. Therefore, the problem of heavy metal pollution needs to be addressed [8].

Wastewater from industrial processes mostly contains two contaminants, one of them heavy metals [9]. The phrase "heavy metal" refers to any metal with an atomic number and density of more than 20 and 5 g/cm^3 , in that order. According to [8], heavy metals include elements such as lead (Pb), mercury (Hg), cadmium (Cd), zinc (Zn), chromium (Cr), arsenic (As), nickel (Ni), and copper (Cu). To address this problem, various methods are applied to reduce the levels of heavy metal pollution in the environment. Commonly used solutions to reduce heavy metal pollution include filtration, evaporation, precipitation, ion exchange, and adsorption. One effective method is the adsorption method, and uses simple absorption, which does not require high operational costs. This adsorption method is often used because it is environmentally friendly and provides maximum results in heavy metal absorption [10].

The type of absorption media or adsorbent is very important in the adsorption process. The selection of adsorption materials also requires in-depth analysis, including raw material prices, characteristics, and the adsorbent's adsorption capacity. Currently, various types of adsorbents are available, some of which tend to be more affordable and offer greater adsorption capacity, and these are continually being sought and further developed. One frequently developed adsorbent is hydroxyapatite. Hydroxyapatite is readily available, both natural and synthetic. The raw material itself is also relatively inexpensive. Its adsorption capacity is biocompatible, bioactive, and bioresorbable. However, in the application process, hydroxyapatite has the disadvantage of frequently forming suspensions and being difficult to separate from the solution. Furthermore, using hydroxyapatite in its sole form also requires a relatively large amount of material. Therefore, hydroxyapatite materials are needed to overcome these shortcomings.

Innovation in hydroxyapatite composites offers a solution to overcome these shortcomings. One approach is the addition of magnesium phosphate (MgPO_4). Magnesium phosphate composites, which are used to form suspended hydroxyapatite, can assist the performance of the suspended hydroxyapatite by separating the absorbed solution. Hydroxyapatite advantages include its environmental friendliness, availability, affordability, and increased adsorption capacity, as magnesium phosphate can enhance hydroxyapatite's high adsorption capacity from green mussels [11]. Therefore, this study, using hydroxyapatite/magnesium phosphate, requires analysis to determine its characteristics, synthesis methods, and adsorption capacity as an adsorbent. This study aimed to synthesis and characterization hydroxyapatite/magnesium phosphate as an adsorbent for wastewater analysis using the precipitation method on green mussel shell waste. The discussion covered the synthesis methods, characterization, and adsorption capacity of the adsorbent for heavy metal adsorption in wastewater [12].

2 Method

2.1 Tool and Material

The tools needed in this research include standard laboratory glassware, oven, stainless steel autoclave tube, hot plate stirrer, magnetic stirrer, XRD (PANalytical X'Pert PRO), XRF (PANalytical Minipal 4), SEM-EDX (FEI Inspect-S50), AAS (ICE™ 3500), FTIR (Shimadzu IRPrestige 21), UV-Vis (Agilent Cary 60) instruments. The materials needed for the research included cleaned green mussel shells, 0.06 M Na₂HPO₄·2H₂O solution (Merck), 25 % MgPO₄ powder (Merck), 0.1 M Na₂EDTA solution (Merck), H₂O₂ 3 % solution (Merck), distilled water, KBr powder (Merck), 96 % ethanol (Smartlab), and filter paper.

2.2 Synthesis of Hydroxyapatite from Green Mussel Shells

Green mussel shells (*Perna viridis*) were collected from the Port of Pasuruan City. Cleaned green mussel shells (*Perna viridis*) were crushed and boiled (5 hours) to remove organics. The green mussel that had been boiled for 6 hours was cleaned using distilled water and soaked in a 3 % H₂O₂ solution for 5 hours. Then rinsed with distilled water and dried for 7 hours in an oven at 100 °C. The dried green mussel shells were weighed and calcined in a furnace with varying temperatures of 800 °C, 900 °C, and 1000 °C for 5 hours. The resulting calcination results were then ground into powder using a mortar and pestle. The calcination product obtained in powder form was dissolved in distilled water and then characterized using an AAS instrument. The product yield from the calcination process was calculated by comparing the change in sample mass to the initial mass using Equation 1 with the following formula:

$$\% \text{Ca(OH)}_2 = \frac{\text{Mass after calcination}}{\text{Mass before calcination}} \times 100 \% \dots\dots\dots(1)$$

Hydroxyapatite synthesis required 50 mL of 0.1 M EDTA solution and 0.06 M Na₂HPO₄·2H₂O solution. In this synthesis, 2.8 grams of CaO were dissolved in 50 mL of 0.06 M Na₂HPO₄·2H₂O solution. Then, 50 mL of 0.1 M Na₂EDTA solution was added to the mixture at a rate of 4 mL/minute. The mixture was stirred for 1 hour at 400 rpm and heated to 100 °C. The resulting precipitate was washed with distilled water until the pH was neutral and dried in an oven at 40 °C for 24 hours to obtain a white powder. The resulting powder was characterized using FTIR and XRD.

2.3 Synthesis of HAp/MgPO₄ Nanocomposites

The synthesis of HAp/MgPO₄ nanocomposites with a 1:1 composition was carried out by dissolving 0.5 grams of MgPO₄ in ethanol with the addition of 0.5 grams of hydroxyapatite powder. The sample mixture was then stirred for 1 hour using a hotplate stirrer at 400 rpm and heated to 130 °C. After the mixing process was completed, the composite powder was formed. The next step was stirring with a magnetic stirrer for 24 hours. The composite powder was separated from the solution and washed with distilled water until the pH was neutral. The composite powder was dried in an oven at 80 °C for 12 hours to obtain the HAp/MgPO₄ nanocomposite. The resulting powder was characterized using FTIR and XRD.

2.4 Characterization of HAp/MgPO₄ Nanocomposite

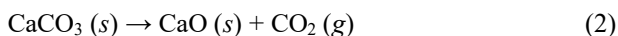
Characterization of hydroxyapatite quantitative include measurement of XRD (crystallinity index, crystallite size, highest peak d-spacing, and 2-theta HAp), XRF (chemical compound content in green mussel shell), SEM (morphology and pore size distribution), FTIR (functional group), AAS (Ca metal content), and UV-Vis (band gap and phosphate absorbance results).

2.5 Data Analyst Technique

The data analysis technique used is quantitative analysis by comparing research results with the literature. XRD for crystallinity index, crystallite size, highest peak d-spacing, and 2-theta HAp, XRF for chemical compound content in green mussel shell, FTIR for functional groups, SEM for morphology and pore size distribution, UV-Vis to identify the concentration of phosphate and band gap, and AAS to identify the concentration of total calcium metal.

3 Result and Discussion

Hydroxyapatite (HAp) has the chemical formula Ca₁₀(PO₄)₆(OH)₂ in its synthesis process requires the main precursors in the form of calcium and phosphate to form a thermodynamically stable crystal structure [13]. Calcium oxide (CaO) plays an important role as a source of calcium in HAp synthesis. In this study, CaO was obtained through the calcination process of green mussel shell waste, which is one of the natural sources of calcium. The calcination process changes the crystal phase in the sample into a more stable phase with high crystallinity, such as CaO [13]. The utilization of green mussel shells waste not only reduces waste, but also produces calcium oxide in a more environmentally friendly way. This is in line with efforts in materials science to find alternative raw materials that are more sustainable, while minimizing negative impacts on the environment through recycling unused organic materials. The content of green mussel shells is 99.5 % calcium carbonate, 0.23 % Sc metal, and 0.47 % Sr metal. In this study, cleaned green mussel shells were then ground and calcined at temperatures of 800 °C, 900 °C, and 1000 °C for 5 hours to decompose organic compounds and calcium carbonate (CaCO₃) into calcium oxide (CaO) by releasing carbon dioxide (CO₂). The calcination result showed that the CaO powder was white with different yields at each temperature at 800 °C (97.32 %), 900 °C (74.53 %), and 1000 °C (74.39 %). This process shows that the higher the calcination temperature, the lower the yield produced, which can be caused by the higher volatility of organic components and deeper decomposition at high temperatures. The reaction equation that occurs during the green mussel shell calcination process is explained in Equation 2.



Green mussel shells were pulverized and calcined at 800 °C, 900 °C, and 1000 °C to break down organic components and calcium carbonate (CaCO₃) into calcium oxide (CaO) by releasing carbon dioxide (CO₂). CaO compound produced from the calcination process is used in the synthesis of hydroxyapatite compounds. CaO is mixed with the EDTA solution which functions as a chelating reagent or complexing reagent [12]. The EDTA solution is around Ca²⁺ to form a Ca-EDTA complex compound. The next step is the addition of Na₂HPO₄·2H₂O solution, which aims to release Ca²⁺ ions from the Ca-EDTA complex. The free Ca²⁺ ions can then interact with OH⁻ ions from the water ionization process, forming a hydroxyapatite structure. In addition, Ca²⁺ ions also bind to phosphate ions (PO₄³⁻) derived from Na₂HPO₄, forming hydroxyapatite crystal nuclei. These crystal nuclei then grow further through a heating process in an oven, which serves to remove water and produce

hydroxyapatite powder in the form of dry deposits. This process allows the formation of stable HAp crystals that can be used for adsorbent applications such as adsorbent material. Green mussel shell samples were characterized using XRF to determine the elemental and compound composition of the green mussel shells before and after calcination. This aimed to determine the percentage of elements and oxides in the green mussel shells by ensuring that the Ca content in the green mussel shells was more dominant or higher than the others. The characterization results are listed in Table 3. The CaO content detected in the green mussel shells after calcination ranged from 98.08 % to 98.59 %. The highest CaO content in the green mussel shells was at 800 °C, with 98.59 %, which has great potential for increasing the adsorbent capacity of HAp/MgPO₄. Before calcination, the CaO content was found to be 96.23 % [14].

Table 3. Comparison of green mussel shells composition before and after calcination at 800-1000 °C.

No	Oxide	Before Calcination	After Calcination (800 °C)	After Calcination (900 °C)	After Calcination (1000 °C)
1.	CaO	96.03 %	98.53 %	98.59 %	98.59 %
2.	Other oxides	3.97 %	1.47 %	1.41 %	1.41 %

The XRF data displayed shows the oxide composition of a sample before and after the calcination process with various temperature variations of 800 °C, 900 °C, and 1000 °C in green mussel shells. The main oxide detected in the sample is CaO and shows a significant increase after calcination at various temperature variations. Table 3. The results show that green mussel shells contain 96.3 % calcium [14]. Before calcination and after calcination it increases to 98.59 % which can produce high calcium oxide. Green mussel shells can be used as a source of calcium in comparison with hydroxyapatite and magnesium phosphate as adsorbent materials. The increase in results from calcination indicates that the calcination process can help decompose organic compounds or impurities, so that it can increase the CaO content in green mussel shell samples.

The AAS test was used to determine the concentration of calcium (Ca) in the calcined filtrate of calcium oxide. The sample used in this test was CaO with a temperature variation of 800 °C, 900 °C, and 1000 °C. The standard curve for calcium metal was $Y = 0.01572x + 0.0011$ with an R^2 of 0.9998. The absorbance and calcium concentration of the green mussel shell hydroxyapatite sample using AAS (Atomic Absorbance Spectroscopy) are as Table 4:

Table 4. Calcium concentration data in calcined CaO

Test	Absorbance (A)	Calcium Concentration (ppm)
HAp 800 °C	1.00	56.69 ± 0,01
HAp 900 °C	2.53	154.05 ± 0,01
HAp 1000 °C	0.91	50.09 ± 0,01

In this study, UV-Vis analysis was used to determine the parameters that affect the stability and purity of the material. In addition, the concentration value (ppm) was measured to see the effect of calcination temperature on the amount of dissolved compounds or residues remaining in the sample. The following table shows the results of UV-Vis testing on HAp samples at three variations of calcination temperatures, namely 800 °C, 900 °C, and 1000 °C. UV-Vis test to determine the wavelength of phosphate (PO₄). The samples used in this test use the filtrate results from the HAp temperature variation of 800 °C, 900 °C, and 1000 °C. The standard curve for calcium metal was $Y = 0.2655x - 0.0092$ with an R^2 of 0.9999. Depicts the differences in phosphate concentration levels using a UV-Vis spectrophotometer as follows Table 5:

Table 5. Depicts the differences in parameter concentration levels using a UV-Vis spectrophotometer

Sample	Absorbance (A)	Concentration (ppm)
HAp 800 °C	1.28	0,332
HAp 900 °C	1.11	0,287
HAp 1000 °C	1.12	0,290

Based on the table shown, the measurement results using a UV-Vis spectrophotometer show variations in absorption values (A) and concentration (ppm) in hydroxyapatite (HAp) samples calcined at different temperatures, namely 800 °C, 900 °C, and 1000 °C. The UV-Vis spectrophotometry technique is used to analyze the sample's ability to absorb light at a certain wavelength, which is related to the number of active species or compounds contained in the HAp dissolution solution. The higher the absorption value, the greater the material's ability to absorb light, which is generally directly proportional to the active species concentration in the solution. In the 800 °C HAp sample, the highest absorption value was recorded at 1.28 with a concentration of 0.332 ppm. This indicates that at a calcination temperature of 800 °C, hydroxyapatite still has a crystal structure that is not completely stable, but its surface is quite active in interacting with UV-Vis light. The high surface activity can be attributed to the presence of a relatively large number of hydroxyl (-OH) groups and a relatively small particle size, resulting in stronger light absorption. When the temperature increases to 900 °C, the absorbance value decreases to 1.11 at a concentration of 0.287 ppm. This decrease can be attributed to increased crystallinity and a decrease in the number of hydroxyl groups due to partial dehydration of the HAp structure. At this temperature, some of the -OH groups are released from the crystal lattice, causing changes in the electronic structure that result in reduced light absorption at UV-Vis wavelengths. In other words, increasing the calcination temperature causes changes in the material's optical properties. Interestingly, at 1000 °C, the HAp absorbance value increases slightly to 1.12, while the concentration increases slightly to 0.290 ppm.

This small increase indicates that at higher temperatures, despite further dehydration, crystal reconstruction also occurs, leading to the formation of a more homogeneous and stable phase such as β -tricalcium phosphate (β -TCP) or an increase in the HAp lattice regularity. This can change the energy band gap, which affects its optical properties. In general, the results show that increasing the calcination temperature affects the crystal structure, crystallinity level, and optical properties of hydroxyapatite. This effect is reflected in fluctuating absorption changes, indicating a transition from a less crystalline phase to a more stable phase. In the application context, these results are important because the optical properties measured by UV-Vis can be used to predict the purity level, structural defects, and thermal stability of HAp, which plays a crucial role in biomedical applications such as bone implants or metal ion adsorbents. Thus, it can be concluded that the UV-Vis spectrophotometer is a sensitive characterization tool for detecting structural and compositional changes due to thermal treatment of HAp. The variation in calcination temperature between 800 °C and 1000 °C shows a direct relationship between changes in crystal structure and optical properties, where the optimum temperature conditions can be adjusted depending on the needs of the material application. AAS test to determine the concentration of calcium metal (Ca) in a filtrate from HAp/MgPO₄ filtration. The sample used in this test uses HAp filtration filtrate with a temperature variation of 800 °C, 900 °C, and 1000 °C. The standard curve for calcium metal was $Y = 0.01572x + 0.0011$ with an R^2 of 0.9998. The difference in calcium concentration using AAS table 2:

Table 6. Data calcium concentration in a filtrate hydroxyapatite

Test	Absorbance	Calcium Concentration (ppm)
HAp 800 °C	5.78 A	361.65 ± 0,01
HAp 900 °C	6.86 A	430.51 ± 0,01
HAp 1000 °C	8.67 A	545.96 ± 0,01

AAS data shows that the calcium concentration in the filtrate increases with increasing calcination temperature, from 361.65 ppm at 800 °C to 545.96 ppm at 1000 °C. The measured absorbance also increases from 5.78 A to 8.67 A, in line with the Lambert-Beer law. This demonstrates a direct relationship between heat treatment temperature and the release of Ca²⁺ ions. Therefore, calcination temperature significantly influences the stability of calcium within the HAp structure. At 800 °C, HAp still retains most of its calcium within its crystal structure. Crystallinity at this stage is not yet fully developed, so the ionic bonding of Ca²⁺ with phosphate remains relatively stable. Consequently, the amount of Ca²⁺ released into the filtrate is lower than at higher temperatures. This indicates that the material is more stable against ionic degradation at lower calcination temperatures.

When the temperature was raised to 900 °C, the Ca²⁺ concentration increased to 430.51 ppm. This increase indicates a phase change or crystal rearrangement that triggers the release of calcium ions. At this intermediate temperature, the more soluble tricalcium phosphate (β -TCP) phase is likely to form. Therefore, the release of Ca²⁺ increases even though the phosphate yield remains relatively stable. At 1000°C, the release of Ca²⁺ reached its highest value of 545.96 ppm with an absorbance of 8.67 A. This may be due to the decomposition of hydroxyapatite into the CaO or TCP phase, which has higher solubility. As a result, more Ca²⁺ ions are released into the solution. This phenomenon indicates that high temperatures accelerate the degradation of the HAp structure. XRD (X-ray Diffraction) is a very effective analysis method in identifying the crystal structure of materials, including hydroxyapatite (HAp) extracted from green mussel shell. It was found that there was a similarity in the XRD spectra, where high intensity indicated a significant level of HAp crystallinity. HAp has a characteristic diffraction pattern according to COD ID number 9011091 (Hydroxyapatite) at 31.76°, 32.19°, 32.89°, 34.06°, 35.45°, 38.16°, with the main index (hkl): (-230), (-131), (-231), (-122). (20). Increasing the temperature causes the peak intensity to increase and the peak width to decrease, which theoretically can increase the crystallinity of HAp. The image shows the X-ray diffraction (XRD) patterns of HAp/MgPO₄ samples calcined at 800 °C, 900 °C, and 1000 °C, compared to the standard hydroxyapatite pattern (COD ID 9011091). In general, the diffraction patterns show that the primary phase formed is hydroxyapatite (HAp), but with differences in peak intensity and sharpness due to the influence of calcination temperature and the presence of substitution or interaction with MgPO₄.

In the HAp/MgPO₄ sample at 800 °C, the diffraction pattern shows relatively broad peaks with low intensity compared to higher temperatures. This indicates that at 800°C, the material is still in a semi-crystalline state or has not yet fully crystallized. The main diffraction peaks appear at 2 θ angles of approximately 25.9°, 31.7°, 32.9°, and 39.8°, which correspond to the typical (002), (211), (300), and (310) crystal planes of hydroxyapatite. The broad peaks reflect the small crystallite size and the high degree of atomic structure disorder. When the calcination temperature is increased to 900°C, the intensity of the main peaks increases significantly and the peak shapes become sharper. This increase indicates that the HAp crystal structure experiences more regular atomic growth and rearrangement. The peaks at 2 θ 31.7 ° and 32.9 ° become more dominant, which is characteristic of the pure hydroxyapatite phase. Furthermore, no additional peaks indicating the formation of other phases are observed, thus indicating high phase purity at 900 °C. At 1000°C, the XRD pattern shows peaks with the highest intensity and maximum sharpness, indicating that the material's

crystallinity has reached its optimum. These results also indicate that hydroxyapatite crystals are fully formed and highly thermally stable. However, at this temperature, it should be noted that some literature indicates the potential for hydroxyapatite to decompose into β -TCP and CaO if heated for too long. This pattern shows no strong indication of the formation of other phases, thus concluding that HAp remains stable up to 1000°C. When compared to the standard pattern COD ID 9011091 (Hydroxyapatite), all samples show excellent peak position agreement. This agreement indicates that the primary phase in all samples is hydroxyapatite. It also confirms that the addition of magnesium phosphate (MgPO_4) does not significantly alter the basic HAp structure but has the potential to improve thermal stability and refine crystallite size. The peak with the highest intensity at around 31.7° indicates a dominant (211) plane orientation, which is characteristic of hexagonal HAp crystals. The dominance of this plane indicates directional crystal growth and increased order of the calcium, phosphate, and hydroxyl atoms within the crystal lattice. Furthermore, the decrease in the peak (FWHM) at high temperatures indicates an increase in crystallite size and reduction in internal crystal stress.

At 800°C, the presence of a weak and broad peak can be attributed to the presence of an amorphous phase due to incomplete decomposition. This is common in synthetic HAp derived from biological materials or chemical precipitation, as organic residues and carbonate groups are still present at these temperatures. When the temperature is increased to 900°C, most of the organic components decompose, and the ions in the lattice begin to organize more stably. The results at 1000°C demonstrate the most ideal material conditions in terms of crystallinity and phase purity. The sharp crystal structure indicates that the calcination process successfully refined the HAp phase without causing degradation. This increased temperature also helps evaporate impurities such as carbonate and nitrate that may have formed during synthesis, resulting in a more homogeneous material. The addition of MgPO_4 is thought to affect crystal growth and the thermal stability of HAp.

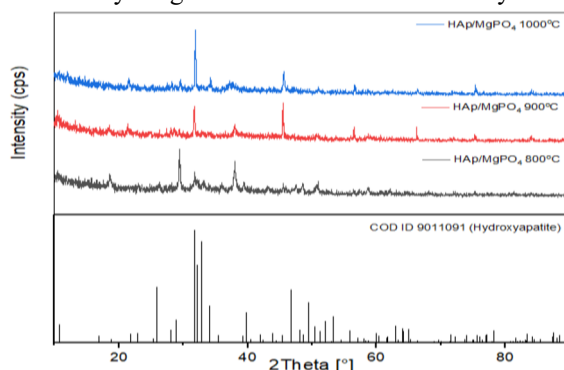


Figure 1. Peak XRD result of HAp/MgPO₄ 800 °C, 900 °C, and 1000 °C

Table 3. XRD analysis results for HAp/MgPO₄ peaks at 800 °C, 900 °C, and 1000 °C

No	Sample	2 θ deg	d(Å)	Crystallinity (%)	Crystalline Size (nm)
1.	HAp/MgPO ₄ 800 °C	29.42°	3.03539	85.488	23.7989
2.	HAp/MgPO ₄ 900 °C	31.71°	2.82129	95.864	27.6968
3.	HAp/MgPO ₄ 1000 °C	31.89°	2.80591	77.457	26.0040

The infrared transmittance spectrum of the HAp/MgPO₄ composite was generated and shown in Figure 2 this spectrum shows the presence of PO₄³⁻ groups detected at several

frequency ranges, namely $1033.85\text{-}1037.63\text{ cm}^{-1}$, $873.75\text{-}877.61\text{ cm}^{-1}$. Meanwhile, carbonate (CO_3^{2-}), which plays an important role in tissue engineering due to its bioactivity and reabsorption properties similar to the composition of human bone, was detected at around 1400 cm^{-1} . The decrease in the intensity of the CO_3^{2-} peak began to occur at a temperature of 1000°C due to carbonate decompose. In addition, in the calcination process at a temperature of 800°C , 900°C , and 1000°C , there was a decrease in the intensity of the OH^- group at around $3500\text{-}3600\text{ cm}^{-1}$, which was caused by the dehydroxylation process of the OH^- group. This shows that the calcination temperature affects the changes in functional groups on adsorbent material [14].

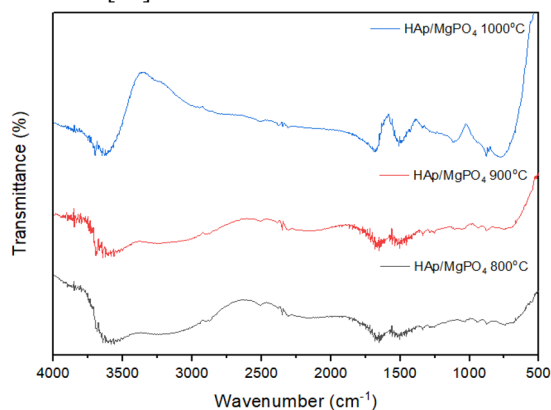


Figure 2. FTIR peak result of HAp/MgPO₄ 800 °C, 900 °C, and 1000 °C

Table 4. FTIR wave number results of HAp 800 °C, 900 °C, and 1000 °C

Vibration	Wavenumber (cm^{-1})				
	HAp/MgPO ₄ 800 °C	HAp/MgPO ₄ 900 °C	HAp/MgPO ₄ 1000 °C	Reference HAp	Ref.
O-H	3645.46 and 3479.58	3523.95 and 3444.87	3630.03 and 3419.79	3634 and 3448	[12]
C-H	2945.30	3030.17	2974.23	-	
-C=O	1990.54	1990.54	1845.87	-	
C=O	1454.32	1454.32	1411.89	1418	[12]
-PO ₄	1033.85 and 877.61	1033.85 and 877.61	1097.5 and 879.54	1045 and 874	[12]

Based on the FTIR results table of HAp/MgPO₄ at various calcination temperatures (800°C , 900°C , and 1000°C), there is a shift and change in the intensity of the absorption band indicating changes in the chemical structure due to the heating temperature. The O–H absorption band appears in the range of $3645\text{-}3419\text{ cm}^{-1}$, consistent with the hydroxyl vibrations in hydroxyapatite (HAp). This value is comparable to the reference (3634 and 3448 cm^{-1}), indicating that the hydroxyl groups are still maintained even though the temperature increases, although there is a slight shift indicating changes in hydrogen bonds or the loss of some OH at high temperatures. The C–H absorption band is detected at $2945\text{-}3030\text{ cm}^{-1}$, which is usually associated with residual organic compounds or carbonate contaminants from the precursor. The presence of this band at high temperatures ($900\text{-}1000^\circ\text{C}$) indicates the possible presence of partial carbonation or impurities, although the intensity tends to decrease with increasing temperature.

Vibrations of the carbonyl group (C=O and -C=O) were detected at $1990\text{--}1845\text{ cm}^{-1}$ and $1454\text{--}1411\text{ cm}^{-1}$. These bands likely originate from carbonate ions (CO_3^{2-}) partially replacing the phosphate groups in the HAp structure (a common phenomenon in hydroxyapatite). The shift of the band to lower wavenumbers at $1000\text{ }^\circ\text{C}$ indicates partial decarbonation due to high temperature, bringing the structure closer to pure HAp. The characteristic phosphate band (PO_4^{3-}) appears at $1033\text{--}877\text{ cm}^{-1}$ and shifts to $1097\text{--}879\text{ cm}^{-1}$ at $1000\text{ }^\circ\text{C}$. This range corresponds to the asymmetric stretching and bending vibrations of PO_4^{3-} , in line with reference literature (1045 and 874 cm^{-1}). The shift towards higher wavenumbers at $1000\text{ }^\circ\text{C}$ indicates increased crystallinity and lattice restructuring due to calcination. Overall, the FTIR data confirm that hydroxyl and phosphate groups remain dominant, with a small reduction in carbonate at high temperatures, thus calcination increases the crystallinity of HAp/MgPO₄.

SEM testing was conducted to determine the surface structure and pore diameter of the HAp sample. The result of the SEM test showed the morphology of the surface structure of the porous hydroxyapatite sample using a calcination temperature variation of $800\text{ }^\circ\text{C}$, $900\text{ }^\circ\text{C}$, and $1000\text{ }^\circ\text{C}$. In the SEM test, it was seen in the hydroxyapatite sample with a temperature variation of $800\text{ }^\circ\text{C}$ (Figure 3), $900\text{ }^\circ\text{C}$ (Figure 7), and $1000\text{ }^\circ\text{C}$ (Figure 11).

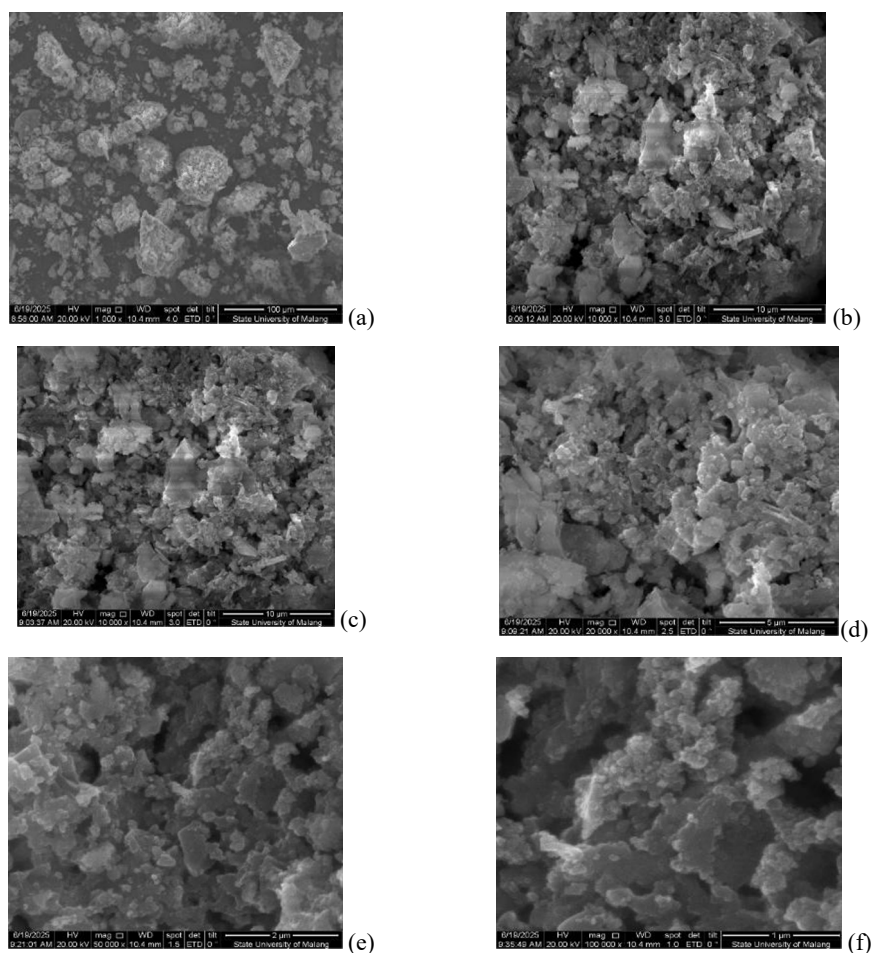


Figure 3. Morphology of hydrothermally synthesized HAp/MgPO₄ $800\text{ }^\circ\text{C}$ with magnifications a) $1.000\times$, b) $10.000\times$, c) $10.000\times$, d) $20,000\times$, e) $50,000\times$, f) $100.000\times$

Figure 3 shows that the calcination temperature can affect the pore diameter size of the hydroxyapatite sample which tends to have porous properties. The pore diameter size of the porous hydroxyapatite sample can be measured using the scale line in the SEM test result image. After measuring the pore diameter on the hydroxyapatite sample, the pore diameter size was obtained with an average of 4-20 nm. The characterization result using SEM at a magnification of 1.000-100.000x visually shows that the morphology formed is a porous material. If observed more closely, it can be seen that the size formed is in the nanometer range. The result of SEM photo observations also show the porosity formed which is irregular and even. Furthermore, the result of SEM-EDX observations show the elements contained in the pure HAp/MgPO₄ sample from green mussel shell. The SEM-EDX result a temperature variation of 800°C Figure 4 (Area 1) and Figure 5 (Area 2)

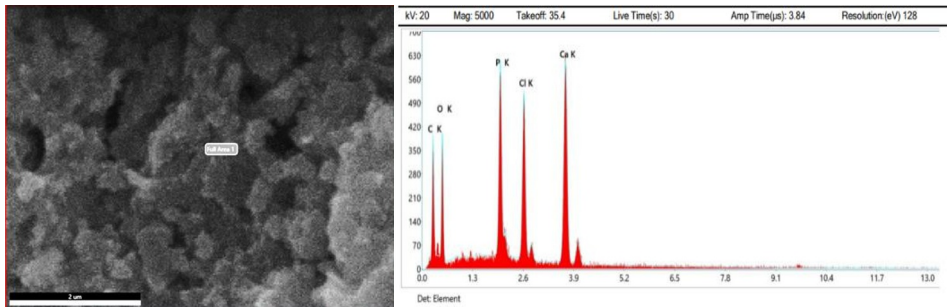


Figure 4. SEM-EDX HAp/MgPO₄ 800 °C result in Area 1

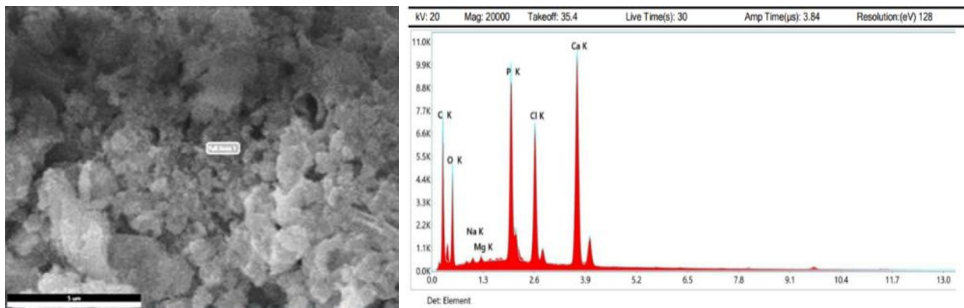


Figure 5. SEM-EDX HAp/MgPO₄ 800 °C result in Area 2

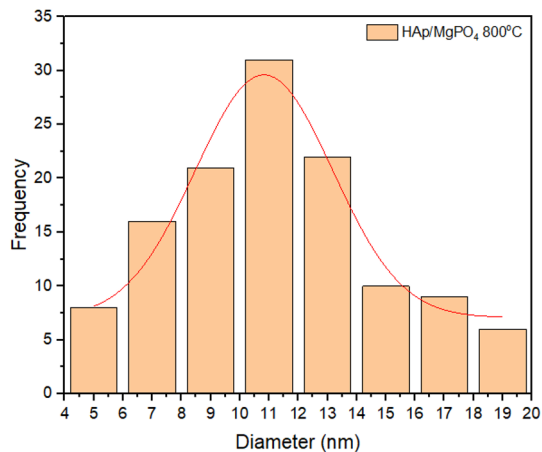


Figure 6. HAp/MgPO₄ 800 °C nanocomposite particle size distribution with 100.000x magnification image

In particle analysis using SEM, ImageJ refracton was performed to determine the particle diameter of the HAp/MgPO₄ nanocomposite. The graph of the results of the SEM analysis performed with ImageJ refracton can be seen in Figure 6. Based on particle testing using SEM with ImageJ refracton, the size of the hydroxyapatite composite in green mussel shell and magnesium phosphate has a composite size range of 4-20 nm, which can be categorized as a nanocomposite. Nanocomposites are materials with a composite size below 100 nm or less than 1 μm . This is supported by reference [15], which defines nanocomposites as composites with a size between 4-20 nm with 100.000x magnification image. The results of the EDX spectrum of HAp in area 1 (Figure 4) show the presence of inorganic elements in the HAp formation consisting of Ca 30.45 %, P 4.47 %, Si 1.26 %, Na 13.68 %, and several organic elements, such as O 50.13 %. The results of the EDX spectrum of HAp in area 3 (Figure 5) show the presence of inorganic elements in the HAp formation consisting of Ca 100 %. These results indicate that in HAp with a temperature variation of 900 °C there is HAp formation content (Ca, P, Si, Na, and O).

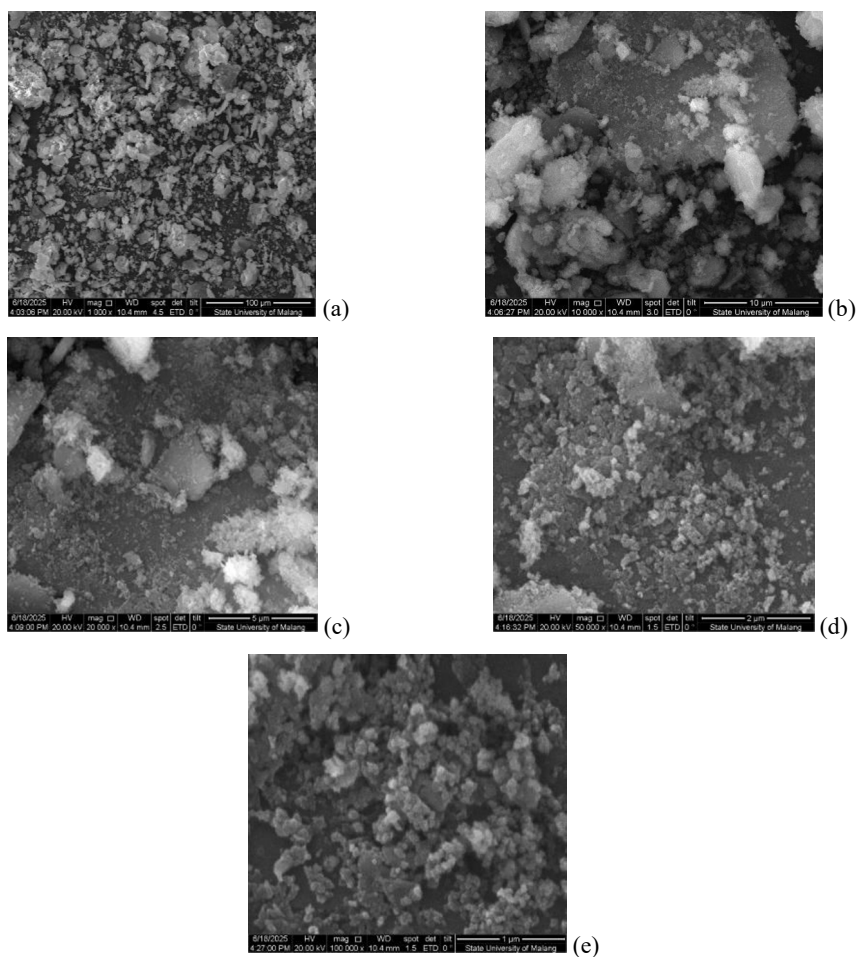


Figure 7. Morphology of hydrothermally synthesized HAp/MgPO₄ 900 °C with magnifications a) 1.000x, b) 10.000x, c) 20,000, d) 50,000x, e) 100.000x

Figure 7 shows that the calcination temperature can affect the pore diameter size of the hydroxyapatite sample which tends to have porous properties. The pore diameter size of the porous hydroxyapatite sample can be measured using the scale line in the SEM test result

image. After measuring the pore diameter on the hydroxyapatite sample, the pore diameter size was obtained with an average of 10-60 nm. The characterization result using SEM at a magnification of 1.000-100.000x visually shows that the morphology formed is a porous material. If observed more closely, it can be seen that the size formed is in the nanometer range. The result of SEM photo observations also shows the porosity formed which is irregular and even. Furthermore, the result of SEM-EDX observations shows the elements contained in the pure HAp/MgPO₄ sample from green mussel shell. The SEM-EDX result a temperature variation of 900 °C Figure 4 (Area 1) and Figure 5 (Area 2)

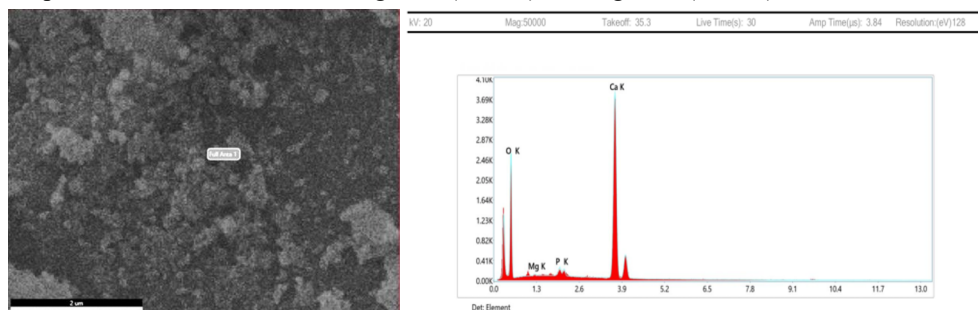


Figure 8. SEM-EDX HAp/MgPO₄ 900 °C result in Area 1

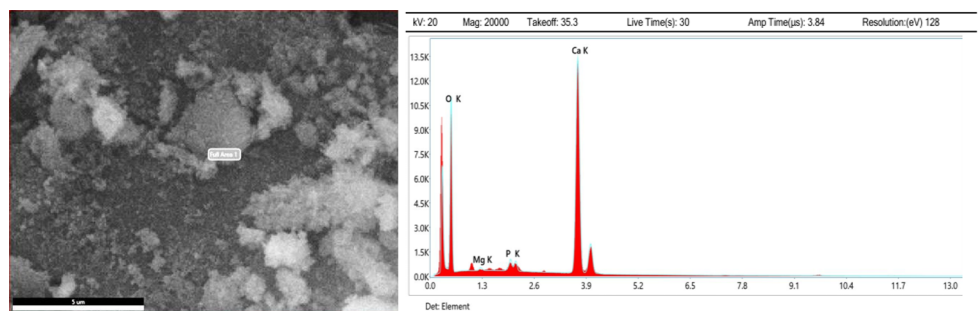


Figure 9. SEM-EDX HAp/MgPO₄ 900 °C result in Area 2

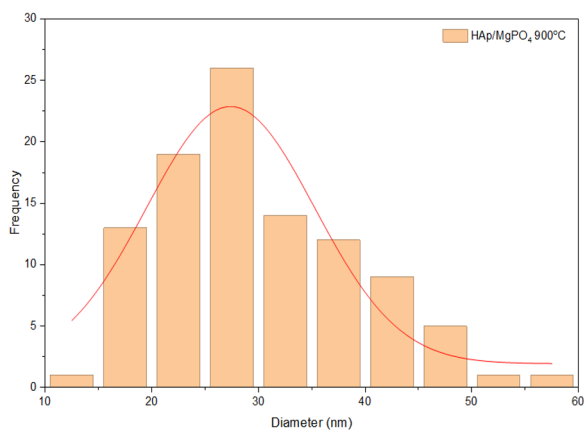


Figure 10. HAp/MgPO₄ 900 °C nanocomposite particle size distribution with 100.000x magnification image

In particle analysis using SEM, ImageJ refraction was performed to determine the particle diameter of the HAp/MgPO₄ nanocomposite. The graph of the results of the SEM analysis performed with ImageJ refraction can be seen in Figure 10. Based on particle testing

using SEM with ImageJ refracton, the size of the hydroxyapatite composite in green mussel shell and magnesium phosphate has a composite size range of 10-60 nm, which can be categorized as a nanocomposite. Nanocomposites are materials with a composite size below 100 nm or less than 1 μm . This is supported by reference [15], which defines nanocomposites as composites with a size between 5-25 nm with 100.000x magnification image. The results of the EDX spectrum of HAp in area 1 (Figure 8) show the presence of inorganic elements in the HAp formation consisting of Ca 33.72 %; P 0.89 %; Mg 0.24 %; and several organic elements, such as O 65.15 %. The results of the EDX spectrum of HAp in area 2 (Figure 9) show the presence of inorganic elements in the HAp formation consisting of Ca 36.51 %, P 0.83 %, P 0.83 %, organic elements such as O 62.49 %, and several elements with low intensity, such as Na 0.2 %; and Mg 0.2 %.

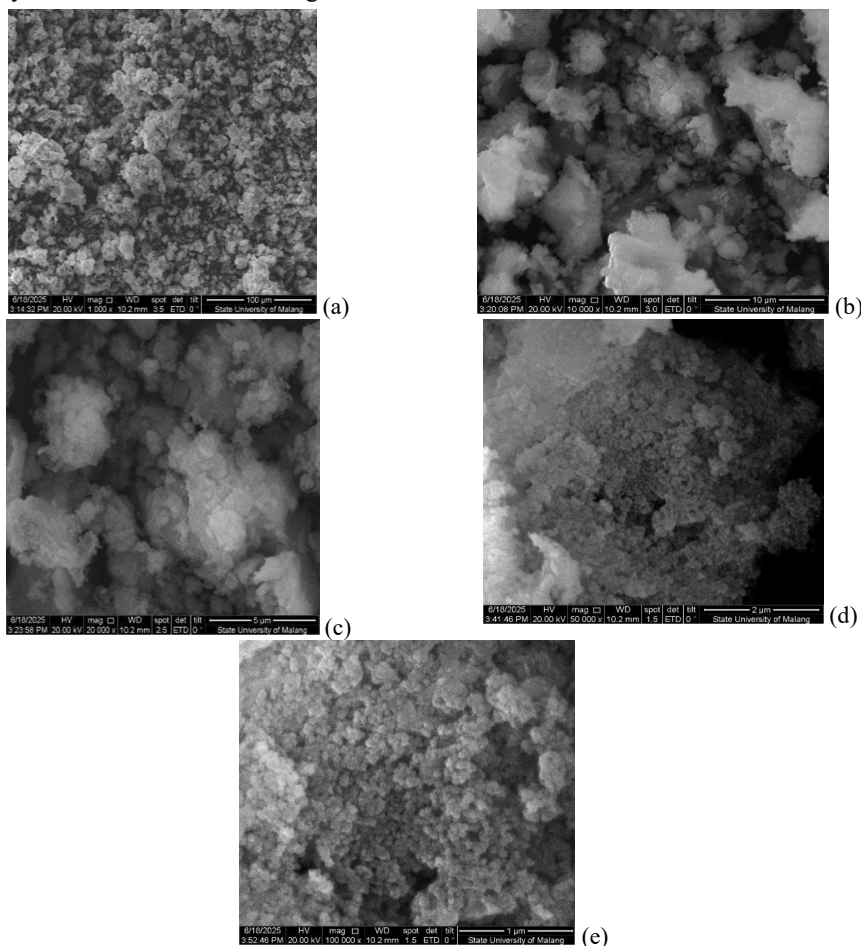


Figure 11. Morphology of hydrothermally synthesized HAp/MgPO₄ 1000 °C with magnifications a) 1.000x, b) 10.000x, c) 20,000, d) 50,000x, e) 100.000x

Figure 11 show that the calcination temperature can affect the pore diameter size of the hydroxyapatite sample which tends to have porous properties. The pore diameter size of the porous hydroxyapatite sample can be measured using the scale line in the SEM test result image. After measuring the pore diameter on the hydroxyapatite sample, the pore diameter size was obtained with an average of 15-100 nm. The characterization result using SEM at a magnification of 1.000-100.000x visually shows that the morphology formed is a porous

material. If observed more closely, it can be seen that the size formed is in the nanometer range. The result of SEM photo observations also shows the porosity formed which is irregular and even. Furthermore, the result of SEM-EDX observations show the elements contained in the pure HAp/MgPO₄ sample from green mussel shell. The SEM-EDX result a temperature variation of 1000 °C Figure 12 (Area 1) and Figure 13 (Area 2)

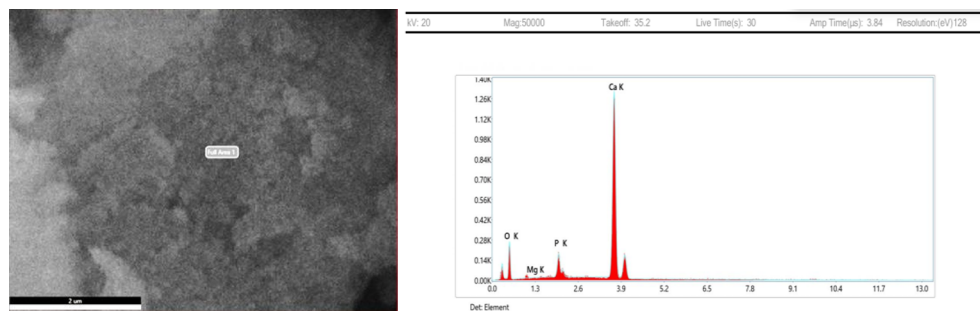


Figure 12. SEM-EDX HAp/MgPO₄ 1000 °C result in Area 1

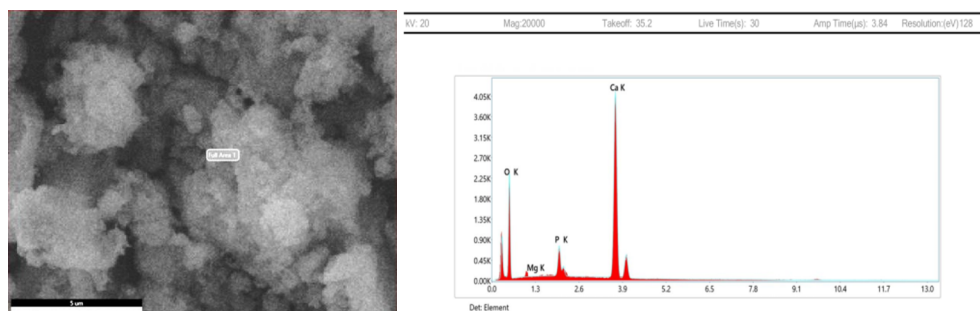


Figure 13. SEM-EDX HAp/MgPO₄ 1000 °C result in Area 2

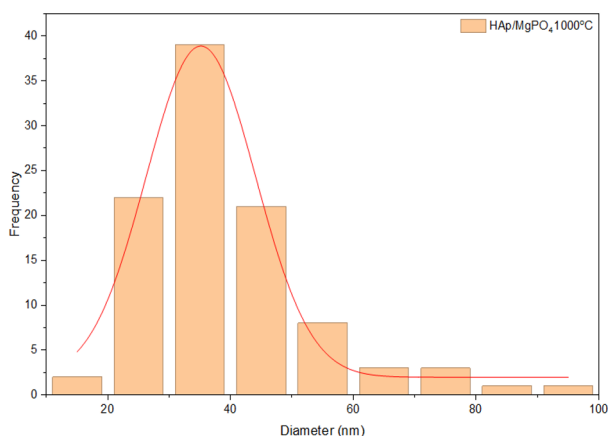


Figure 14. HAp/MgPO₄ 1000 °C nanocomposite particle size distribution with 100.000x magnification image

In particle analysis using SEM, ImageJ refracton was performed to determine the particle diameter of the HAp/MgPO₄ nanocomposite. The graph of the results of the SEM analysis performed with ImageJ refracton can be seen in Figure 14. Based on particle testing using SEM with ImageJ refracton, the size of the hydroxyapatite composite in green mussel shell and magnesium phosphate has a composite size range of 15-100 nm, which can be categorized as a nanocomposite. Nanocomposites are materials with a composite size below

100 nm or less than 1 μm . This is supported by reference [15], which defines nanocomposites as composites with a size between 15-100 nm with 100.000x magnification image. The results of the EDX spectrum of HAp in area 1 (Figure 8) show the presence of inorganic elements in the HAp formation consisting of Ca 55.01 %, P 3.52 % and several organic elements, such as O 41.47 %. The results of the EDX spectrum of HAp in area 2 (Figure 9) show the presence of inorganic elements in the HAp formation consisting of Ca 38.22 %, P 3.19 %, organic elements such as O 58.59 %, and several elements with low intensity such as Na 0.2 %; and Mg 0.2 %. These results indicate that in HAp with a temperature variation of 1000 °C there is HAp formation content (Ca, P), as well as organic content (O).

4 Conclusion

This study successfully synthesized material hydroxyapatite/magnesium phosphate (HAp/MgPO₄) nanocomposites by utilizing green mussel shell waste as a source of biogenic calcium through a precipitation method. The results of the analysis showed that the calcination temperature plays a crucial role in crystal formation; a temperature of 900 °C was identified as the optimal temperature that produced the highest crystallinity of 95.86%. Structurally, FTIR analysis confirmed the formation of typical hydroxyapatite functional groups such as phosphate (PO₄³⁻) and hydroxyl (OH⁻), while SEM-EDX analysis showed a morphology in the form of porous aggregates with nanometer-scale particle sizes (4-100 nm). Increasing the temperature to 1000 °C tended to increase the crystal size but began to show indications of structural degradation characterized by changes in the level of calcium release in the filtrate. Material HAp/MgPO₄ has great potential as an effective adsorbent for wastewater treatment, especially in absorbent heavy metals. This potential is supported by the pore structure and surface area resulting from the nanocomposite synthesis process, which allows for optimal interaction with contaminants. The addition of magnesium phosphate (MgPO₄) to the hydroxyapatite structure aims to overcome the weakness of pure HAp which is often difficult to separate from the solution (forming a suspension) with the presence of this composite, the process of separating the adsorbent from wastewater becomes easier. In addition to its technical effectiveness, the use of green mussel shell waste makes this material environmentally friendly solution (green chemistry).

Acknowledgement

We would like to acknowledge and thank the (1) Central Laboratory of State University of Malang, (2) The authors acknowledge and thank the internal funding at Universitas Negeri Malang for the research funding student innovation 24.2.879/UN32.14.1/LT/2025.

References

1. Vaishali, A. Bendi, S. Singh, and R. Pundeer, "Nano-hydroxyapatite (n-HAp) and its composites for heavy metal removal from water: A comprehensive review," *Next Nanotechnology*, vol. **9**, p. 100339, Jun. 2026, doi: 10.1016/j.nxnano.2025.100339.
2. M. S. Khan, S. Rana, A. Al Mamun, S. A. Shimul, A. Sarkar, and Sk. Ahmad Al Nahid, "Seafood safety concerns: Human health risks from heavy metal bioaccumulation in crustaceans from Cox's Bazar, Bangladesh," *Journal of Food Composition and Analysis*, vol. **151**, p. 108928, Mar. 2026, doi: 10.1016/j.jfca.2026.108928.

3. A. Esmacili Nasrabadi and Z. Bonyadi, "Heavy metal accumulation and human health risks associated with used automotive oil filters," *Environmental Challenges*, vol. **22**, p. 101395, Mar. 2026, doi: 10.1016/j.envc.2025.101395.
4. A. Li, Y. Peng, S. Yao, L. Zhang, and F. Meng, "Research on the application of machine learning in optimizing the heavy metal adsorption of algae-based adsorbents," *Algal Res.*, vol. **94**, p. 104528, Mar. 2026, doi: 10.1016/j.algal.2026.104528.
5. D. R. Kandel, P. Gaudel, M. B. Poudel, W. Yun, and J. Lee, "Single- and multi-metal engineered, functionalized hybrid biochars for heavy metal adsorption: synthesis, structure-function relationships, and coordination mechanisms," *Coord. Chem. Rev.*, vol. **555**, p. 217521, May 2026, doi: 10.1016/j.ccr.2025.217521.
6. W. Li, X. Cui, R. Jing, Q. Zhang, T.-T. Lim, and G. Qian, "Green synthesis of binder-free waste-derived adsorbent for H₂S removal at ambient temperature," *J. Environ. Chem. Eng.*, vol. **13**, no. 6, p. 119618, Dec. 2025, doi: 10.1016/j.jece.2025.119618.
7. S. Kotnala *et al.*, "Impact of heavy metal toxicity on the human health and environment," *Science of The Total Environment*, vol. **987**, p. 179785, Jul. 2025, doi: 10.1016/j.scitotenv.2025.179785.
8. X. Ren, D. Fan, J. Mao, P. Cheng, X. Zhang, and X. Sun, "Response of high-resolution heavy metals records to human activities after considering the influence of early diagenesis in the East China Sea over the last 70 years," *Cont. Shelf Res.*, vol. **298**, p. 105638, Apr. 2026, doi: 10.1016/j.csr.2026.105638.
9. B. Bouzar, N.-E. Abriak, and M. Benzerzour, "Sustainable reuse of mineral waste: Synthesis and comprehensive characterization of hydroxyapatite (HAP)," *Green Technologies and Sustainability*, vol. **4**, no. 2, p. 100315, Apr. 2026, doi: 10.1016/j.grets.2025.100315.
10. Charlena, Nazriati, B. Marita Soebrata, and M. Dicky Iswara, "Synthesis and Characterization of Hydroxyapatite Composites Based on Tutut (*Belamyia Javanica*) and Magnetite by Coprecipitation as Adsorbents of Pb Metals Ion," *Science and Technology Indonesia*, vol. **10**, no. 1, pp. 111–122, Jan. 2025, doi: 10.26554/sti.2025.10.1.111-122.
11. J.-Y. Hou, X.-J. Fu, and X. Ren, "Mollusk Shells as Marine Bioactive Materials: Composition, Bioactivities, and Prospects for Food and Health Applications," *iScience*, p. 114748, Jan. 2026, doi: 10.1016/j.isci.2026.114748.
12. Wulandari, D. V. Wellia, and N. Jamarun, "The calcination temperature effect on the crystallization and morphology of hydroxyapatite from bamboo shell (*Sollen spp.*)," 2023, p. 020016. doi: 10.1063/5.0114309.
13. J. Wang, M. Ge, H. Wang, H. Yao, Y. Deng, and J. Wei, "Mussel-inspired novel coating with cariogenic biofilm inhibition and *in situ* remineralization properties for caries treatment," *Mater. Adv.*, vol. **6**, no. 3, pp. 1067–1074, 2025, doi: 10.1039/D4MA01160K.
14. A. R. Liandi, R. W. Sari, T. P. Wendari, Imelda, D. Febriantini, and A. Insani, "Hydroxyapatite/PCL/Fe₃O₄ waste-based composite: An efficient green catalyst for spirooxindole-chromene synthesis under ultrasonic irradiation," *Case Studies in Chemical and Environmental Engineering*, vol. **10**, p. 100892, Aug. 2024, doi: 10.1016/j.cscee.2024.100892.
15. F. Shafiq *et al.*, "Charge transformation of hollow mesoporous hydroxyapatite (HM-HAP) and its application in the efficient removal of anionic dyes," *Microporous and Mesoporous Materials*, vol. **399**, p. 113852, Jan. 2026, doi: 10.1016/j.micromeso.2025.113852.